Journal of Applied Polymer Science

Synergistic Effect of Aluminum Hydroxide and Nanoclay on Flame Retardancy and Mechanical Properties of EPDM Composites

Ynh-Yue Yen,[1] Hsin-Ta Wang,[1] Wen-Jen Guo[2]

[1]Institute of Organic and Polymeric Materials, National Taipei University of Technology, Taipei 106, Taiwan

[2]Department of Chemical Engineering and Biotechnology, Institute of Chemical Engineering, National Taipei University of Technology, Taipei 106, Taiwan

Correspondence to: H. T. Wang (E-mail: htwang@ntut.edu.tw)

ABSTRACT: The composites based on ethylene–propylene–diene monomer rubber (EPDM) with aluminum hydroxide (ATH), nanoclay, vulcanizing agent, and curing accelerator were prepared by conventional mill compounding method. The thermal stability and the flame retardant properties were evaluated by thermogravimetric analysis (TGA), limiting oxygen index (LOI), UL-94 test, cone calorimeter, and smoke density chamber tests. The results indicated that the substitution of the nanoclay in the EPDM/ATH composites increased the 50% weight loss temperature and the LOI value, and reduced the peak heat release rate (pk-HRR), the extinction coefficient (Ext Coef), the maximal smoke density (Dm), and the whole smoke at the first 4 min (VOF4) of the test specimens. The synergistic flame retardancy of the nanoclay with ATH in EPDM matrix could imply that the formation of a reinforced char/nanoclay layer during combustion prevents the diffusion of the oxygen and the decomposed organic volatiles in the flame. The mechanical properties of the composites have been increased by replacing more of the nanoclays into the EPDM/ATH blends. The best loading of the nanoclay in EPDM/ATH composites is 3 wt %, which keeps LOI in the enough value, the V-0 rating in the UL-94 test, and the improved mechanical properties with better dispersion and exfoliation of the nanoclays shown by transmission electron microscopy (TEM) micrographs. © 2013 Wiley Periodicals, Inc. J. Appl. Polym. Sci. 130: 2042–2048, 2013

KEYWORDS: clay; composites; rubber; flame retardance; thermosets

Received 7 December 2012; accepted 9 April 2013; Published online 14 May 2013

DOI: 10.1002/app.39394

INTRODUCTION

Ethylene–propylene–diene monomer rubber (EPDM) is used in many fields including construction, automobile manufacture, and electrical insulation. By virtue of various advantageous features such as excellent thermal stability, weathering resistance, flexibility at low temperature, good chemical resistance especially to polar media, excellent high resistivity, low dielectric constant, and ease of fabrication and processing, EPDM is widely applied in the wire and cable industry.[1–6] However, EPDM is extremely flammable, and flame retardant agents must be added to reduce the flammability of EPDM. Synergistic flame retardants such as antimony trioxide and halogen-containing compounds are often added to EPDM composites to improve the flame retardancy, but such retardants, especially halogen-typed materials, would produce toxic or corrosive substances on burning, and this causes the health and environmental risks.

The use of the halogen-free fire retardant compounds is an alternative to both the halogenated and inorganic flame retardants. A well-known flame retarder and smoke suppressor is aluminum hydroxide (ATH), whose main advantage over other similar agents is its low cost and negligible toxicity. ATH on burning builds up a protective aluminum oxide layer cutting down the supply of oxygen and the decomposed organic products into combustion zone. Also, the water molecules produced during the decomposition of ATH lower down the temperature of the burning surface. Both processes would retard the flame and the smoke and eventually stop the combustion.

In literature, the flame retardancy and the smoke suppression of EPDM with ATH have been reported.[7–11] In order to get the effective flame retardancy, the ATH must be added into the material with a sufficient amount (>50 wt %), and this could cause decrease in some of the physical and mechanical properties of the composites.[7,8]

The addition of the nanoclay into polymers has been identified that the composite can increase in some extent of thermal stability, flame retardancy, mechanical property, and the capability of smoke suppression.[12–19] Very limited studies have been done on the addition of the nanoclay into EPDM rubber as a flame

retardant additive.[14,20–22] Some aspects, like the best amount of the nanoclay, and some contrary facts in the flammability and smoke tests, deserve to be studied.

This work is mainly devoted to study the synergistic flame retardant effect of ATH with the nanoclay for EPDM blends using thermogravimetric analysis (TGA), limiting oxygen index (LOI), UL-94 test, transmission electron microscopy (TEM) characterization, cone calorimeter test, and smoke density chamber test. Meanwhile, the amount of the nanoclay to be the most effective to inhibit the flame and the smoke properties of the thermosetting EPDM composites has been investigated.

EXPERIMENTAL

Materials

Ethylene–propylene–diene terpolymer (Vistalon™ 5601), consisting of 68.5 wt % ethylene and 5.0 wt % 5-ethylidene-2-norbornene, was supplied by Exxon Co. The pristine nanoclay (PK-812), a natural montmorillonite (MMT) with a cation-exchange capacity of 94 meq/100g was obtained from Pai Kong Co. (Taiwan). It was ion-exchanged by octadecylamine in acidic condition at 80°C for 1 h and thereafter used in all this study. The ATH (H-42M) was supplied by Showa Denko Co. (Japan), with a median particle size of 1.0 μm and a specific surface area (BET) of 5.0 m^2/g. The vulcanizing agent, sulfur (Struktol SU135 containing 75 wt % sulfur) was bought from Symtake Chemical Co. (Taiwan). The vulcanizing accelerator, tetramethylthiuram monosulfide (TS) was provided by Shanghai Chemson Chemicals Co. (China).

Preparation of Composites

First, EPDM and the nanoclay were mixed in a Barbender (Atlas, PLE-331) with a rotation speed of 40 rpm for 20 min at a temperature of 120°C. Then, the EPDM/nanoclay mixture, a desired amount of ATH, sulfur (1 phr) and TS (1.5 phr) were mixed on a 6″ two-roll mill (Yow Chuan Co., Taiwan), with a rotation speed of 32 rpm for 10 min. After sufficient mixing, the material was hot-pressed at 100 MPa and 175°C for 15 min (complete vulcanization) into sheets with a suitable thickness. The compositions of EPDM/ATH composites are listed in Table I.

Characterization of Composites

TGA Analysis. The thermogravimetric measurements were performed on a TGA Q50 (TA Instruments) analyzer at a heating rate of 20°C/min from 30 to 600°C. EPDM, EPDM/ATH, and EPDM/ATH/nanoclay composites were examined under an air flow with sample size 10–15 mg.

Table I. Compositions of All Samples (wt %)

Code[a]	EPDM	ATH	Nanoclay
EPDM	100	0	0
EPDM/ATH	50	50	0
EPDM/ATH/C1	50	49	1
EPDM/ATH/C2	50	48	2
EPDM/ATH/C3	50	46	3
EPDM/ATH/C6	50	44	6

[a] Each sample contains sulfur 1 phr and TS 1.5 phr.

LOI Analysis. LOI values were measured using an ON-1 test instrument (Suga Test Instrument Co., Japan) on the specimens of 100 × 6.5 × 3 mm^3 according to the standard limiting oxygen index test ASTM D2863-77.

UL-94 Test. The UL-94 tests were executed to evaluate the flame speed of test specimens in atmosphere. An SB-94L type instrument (Sin Fair Electric Co., Taiwan) was applied to the sheets of 120 × 13 × 3 mm^3 according to the standard UL-94 test ASTM D635-77.

Cone Calorimeter Test. Cone calorimeter experiment was operated on an Atlas CONE 2 instrument at an incident heat flux of 50 kW/m^2. The ASTM E1354 standard was used. The heat release rate (HRR) was examined for EPDM and EPDM/ATH composite specimens of 100 × 100 × 6 mm^3 size. The HRR curve obtained consists of the peak heat release rate (pk-HRR), the time for ignition of the specimen, the total heat release, and the time for sustained ignition. In cone calorimeter test, the extinction coefficient (Ext Coef) is another important parameter to represent the amount of smoke produced from the material during combustion.

Smoke Density Chamber Test. A smoke density chamber tester, NBS type (Fire Testing Technology, UK) was applied to measure the specific optical density of smoke (Ds) of the EPDM composite under a smoldering process. The small furnace was set so that the sample received 2.5 W/cm^2 thermal energy. Specimens were 75 × 75 × 2.5 mm^3 size according to the ASTM E662 standard. The maximal smoke density (Dm) was obtained from Ds curve for each sample. The smoke properties for each specimen can be defined as follows:

1. Ds(t)-specific optical smoke density at time t.

$$\mathrm{Ds}(t)=132\times\log\frac{100\%}{T(t)} \tag{1}$$

Where $T(t)$ is the light transmission (%) at time t and 132 is the factor resulting from the volume of the light beam and the exposed specimen surface area.

(2) VOF4- integral of the Ds(t) curve calculated from $t = 0$ to $t = 4$ min

$$\mathrm{VOF4}=\sum_{n=0}^{n=3}\frac{\Delta t[\mathrm{Ds}(n)+\mathrm{Ds}(n+1)]}{2}, \tag{2}$$

Where the trapezoid rule was used with the time interval $\Delta t =$ 1 min.

TEM Characterization. TEM images were obtained on a JEM-1230 (JEOL, Japan) in order to obtain the dispersion and exfoliation of the nanoclays inside the compounded composite.

Mechanical Properties Test. The tensile properties, ultimate tensile strength and elongation at break, were determined using a Monsanto tensile tester (Tensometer 10) according to the ASTM D638 standard with a crosshead speed of 500 mm/min at 25 ± 2°C. All measurements were made for each sample with five specimens at least in order to get the reproducible average values.

Applied Polymer SCIENCE

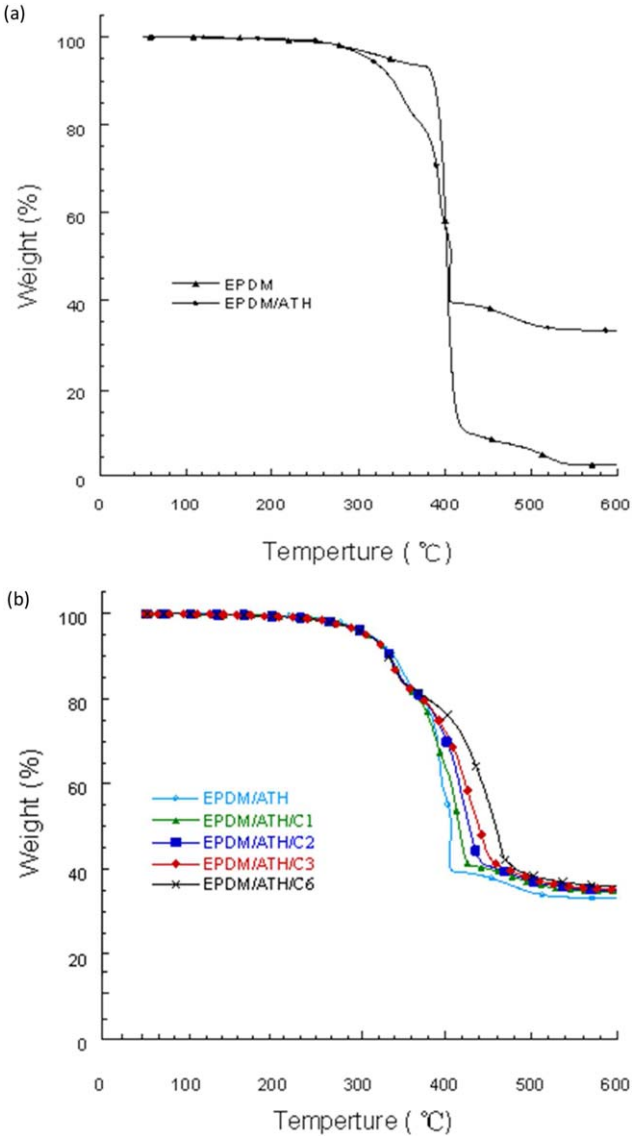

Figure 1. TGA curves of (a) EPDM and EPDM/ATH (b) EPDM/ATH composites. [Color figure can be viewed in the online issue, which is available at wileyonlinelibrary.com.]

RESULTS AND DISCUSSION

Thermal Stability

The TGA curves of EPDM and EPDM/ATH are shown in Figure 1(a). In the curve for EPDM/ATH composite, the starting decomposition temperature of material is around 250°C, which is the onset of ATH decomposition.[23] Although the 15% weight loss temperature of EPDM/ATH is lower than that of EPDM (Table II), the 50% weight loss temperature of EPDM/ATH is higher than that of EPDM, and this means that in the temperature range, 250–350°C, the majority of decomposition is from ATH and that the dehydration of the ATH forms an aluminum oxide char layer to slow down the decomposition of EPDM matrix and the process of building the insulating barrier is time-depended. The char yield difference at 600°C between EPDM and EPDM/ATH (Table II) can support above explanation.

Table II. TGA Results of EPDM and EPDM/ATH Composites

Sample	15% Weight loss temperature (°C)	50% Weight loss temperature (°C)	Char yield (%)
EPDM	392	402	2.5
EPDM/ATH	352	406	33.0
EPDM/ATH /C1	348	416	34.5
EPDM/ATH /C2	348	428	34.8
EPDM/ATH /C3	346	439	35.1
EPDM/ATH /C6	346	459	35.7

TGA thermograms for EPDM/ATH composites with varying amounts of the nanoclays (1–6 wt %) are shown in Figure 1(b). Above 400°C, TGA curve moves towards high temperature as the nanoclay content in the composite increases. In Table II, the 50% weight loss temperature of the EPDM (50 wt %)/ATH (50 wt %) is 406°C and is 4°C above the 50% weight loss temperature of the EPDM. The EPDM/ATH/C1 with only 1 wt % nanoclay inside the composite would give a 50% weight loss temperature, 416°C, and this is 10°C above the 50% weight loss temperature of the EPDM/ATH. As the more nanoclay is in the blend, the higher 50% weight loss temperature is. The presence of the nanoclay inside EPDM/ATH composite increases the thermal stability of the material. This phenomenon has been related to the generation of a reinforced aluminum oxide barrier which more effectively blocks the diffusion of oxygen and the decomposed organic volatiles.[15,18] Similar results have been obtained for other materials.[12,19]

In Table II, the char yield at 600°C for EPDM/ATH/nanoclay composite is slightly higher than that of EPDM/ATH. The existence of a small amount of nanoclay (<6 wt %) would promote the production of char and cause the increase in the thermal stability of the EPDM composite.

Flammability Studies

LOI and UL-94 Analyses. Table III lists the LOI and UL-94 data for EPDM, EPDM/ATH, and EPDM/ATH/nanoclay. The LOI values of EPDM and EPDM/ATH are similar to those reported in literature.[7,8] Although the large increase (from 19 to 25) of the LOI value is due to the presence of ATH inside the composite, the existence of the nanoclay inside the composite also causes the increase of the LOI value (from 25 to 27). The LOI value depends on the composition of the EPDM/ATH/

Table III. Combustion Properties of EPDM and EPDM/ATH Composites

Sample	LOI	UL-94
EPDM	19	-
EPDM/ATH	25	-
EPDM/ATH/C1	26	-
EPDM/ATH/C2	27	V-0
EPDM/ATH/C3	27	V-0
EPDM/ATH/C6	26	-

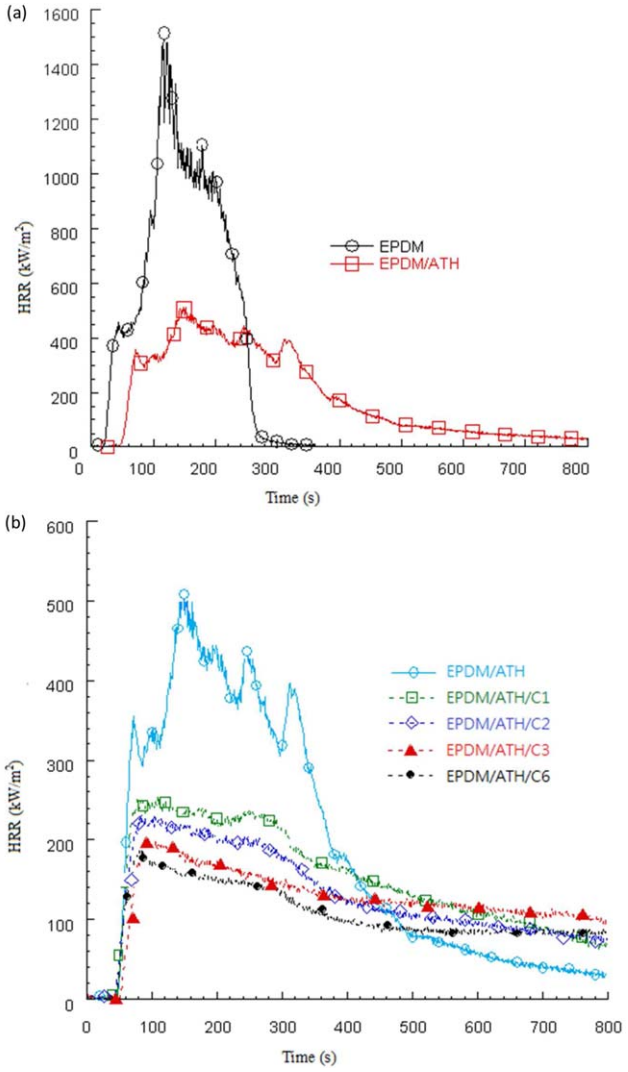

Figure 2. HRR curves of (a) EPDM and EPDM/ATH (b) EPDM/ATH composites. [Color figure can be viewed in the online issue, which is available at wileyonlinelibrary.com.]

nanoclay composite. It ascends gradually to 27 with the increase of the loading of the nanoclay (2–3 wt %) in the blend. As the replaced amount of the nanoclay inside the composite reaches 6 wt %, the LOI value declines to 26. Dispersion and exfoliation of the nanoclays inside the composites are related to this and will be discussed as follows.

The UL-94 vertical burning test results show that the specimen could pass the V-0 rating with replacement of only 2 or 3 wt % of the nanoclay in EPDM/ATH composite.

Cone Calorimeter Analysis. Cone calorimeter tests were conducted on EPDM, EPDM/ATH, and EPDM/ATH/nanoclay. The HRR curves are depicted in Figure 2(a). It can be found that the EPDM sample ignites after 33.6 s in the fast burning mode, and its pk-HRR value 1510 kW/m^2 appears at 122 s after the combustion of the specimen. The addition of ATH in EPDM material causes the ignition time delaying to 53.4 s. The ATH releases water and transforms into aluminum oxide before ignition during heating and therefore the temperature of the tested composite sample is lowered increasing ignition time. The pk-HRR also descends to a value of 512 kW/m^2, which is a reduction of about 66% comparing to that of EPDM. The flatten top of the HRR curve for EPDM/ATH contrasting the sharp peak in HRR curve for EPDM indicates the formation of an aluminum oxide layer and the restriction of the combustion process.[18,19]

At cone calorimeter measuring condition (heat flux of 50 kW/m^2), the ignition times of the EPDM/ATH and EPDM/ATH/nanoclay are similar in Figure 2(b), indicating the nanoclay does not decompose, and it accompanies the ATH in the latter ignition stage to promote the fire retardancy of the composite material. The same kind of phenomenon has been reported in literature.[24] The HRR curves for different compositions of EPDM/ATH/nanoclay composites are shown in Figure 2(b). The pk-HRR value of EPDM/ATH/nanoclay composite is lower comparing to that of EPDM/ATH. When the nanoclay content in the composite is increased, the pk-HRR value decreases from 240 to 180 kW/m^2. In addition, the slope of HRR curve of EPDM/ATH/nanoclay exhibits a progressive decline after reaching the pk-HRR.

The improvement in HRR result suggests that the substitution of the nanoclay to the EPDM/ATH composite would promote the formation of a stacked aluminum oxide layer during the burning of the material. The insulating layer performs not only as a barrier to oxygen supply and heat conduction but also as a suppressor to the release of flammable gases.

Ext Coef curves of EPDM and EPDM/ATH are displayed in Figure 3(a). The EPDM gives much higher value (5.8 L/m) of the Ext Coef relative to that (2.3 L/m) of EPDM/ATH blend. All the Ext Coef curves for EPDM/ATH/nanoclay composites, shown in Figure 3(b), give a steep hill as the ignition of the specimen has just begun. This can be attributed to the release of the volatile gas of EPDM, water vapor (from ATH) and the decomposed products of the organic modifier in the clay. After the rise, the curve of Ext Coef tends to decline slowly for the EPDM/ATH/nanoclay composite and the sample with higher nanoclay content gives the lower emission of smoke during combustion. It can be seen that the variation of the Ext Coef with time is very similar to the change of the HRR of the corresponding material shown in Figure 2(b). It implies that the heat and the smoke are prohibited by the same kind of mechanism. When the ATH is introduced into EPDM, the ATH would build up the fire retardant system, and when the nanoclay accompanies the ATH, the synergistic flame retardancy of the polymer composite can be created.

Smoke Density Chamber Analysis. Figure 4 shows the smoke cdensity curves of EPDM/ATH and EPDM/ATH/nanoclay composites. These curves exhibit a long and slow smoke emittng process with the Dm appearing almost at the end of the measuring time (1200 s) and the VOF4 value only reaching low level, 32–50 (Table IV). The smoke-depression from above materials can be explained that ATH, nanoclay, and EPDM are vulcanized to become a cross-linked matrix and then create a more compact insulating layer during the burning and stop the decomposed volatile products out of the combustion front.

Applied Polymer SCIENCE

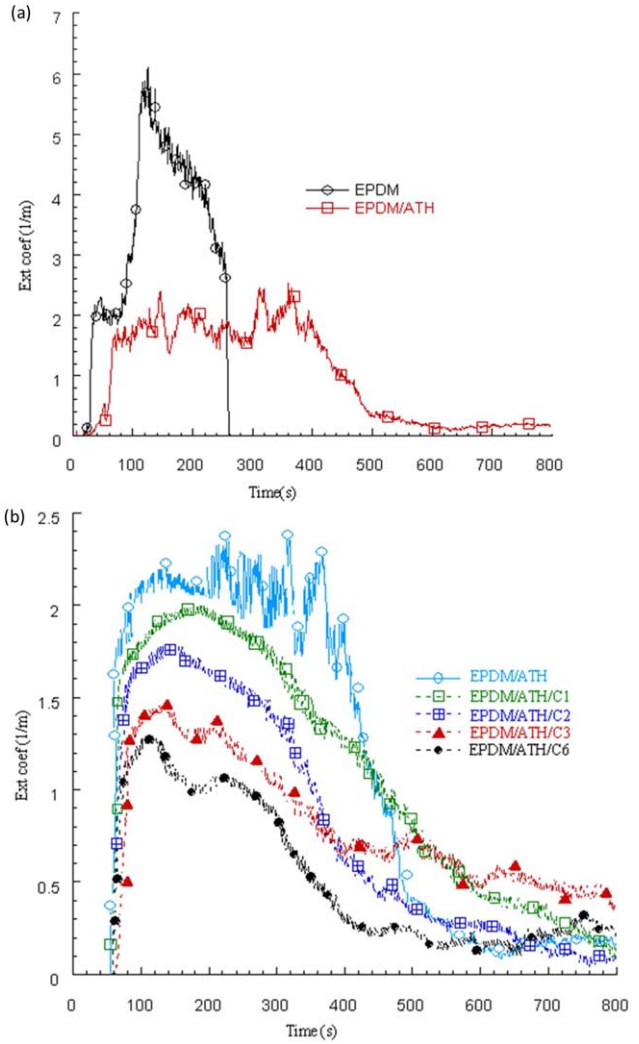

Figure 3. Extinction coefficient curves of (a) EPDM and EPDM/ATH (b) EPDM/ATH composites. [Color figure can be viewed in the online issue, which is available at wileyonlinelibrary.com.]

The increase of the nanoclay in EPDM/ATH/nanoclay composite would reduce Dm. When 3 wt % of the nanoclay exists in the composite, the VOF4 reduces to a minimal value of 32

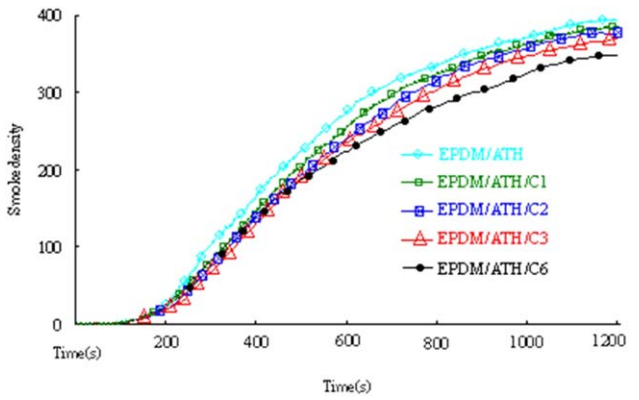

Figure 4. Variation of smoke density with time for EPDM/ATH composites. [Color figure can be viewed in the online issue, which is available at wileyonlinelibrary.com.]

Table IV. Dm and VOF4 of EPDM/ATH Composites

Sample	Dm	VOF4
EPDM/ATH	394	50
EPDM/ATH/C1	384	42
EPDM/ATH/C2	378	38
EPDM/ATH/C3	370	32
EPDM/ATH/C6	349	49

relatively lower than that of EPDM/ATH (Table IV). As the burning of the composite is started, the incinerated products mainly based on aluminum oxide, appear on the surface and form a structured barrier layer. The formed char layer might be easily destroyed by the rapid release of a large amount of heat generated in the beginning of the combustion, thus exposing the lower layer materials to the flame and keeping the ablaze process continuing. As there is enough nanoclay (2–3 wt %) replacement in the EPDM/ATH, the combustion front barrier layer is reinforced by the well-dispersed nanoclay materials and hence would not collapse. Therefore, a higher LOI value is achieved.

The EPDM/ATH/nanoclay composite with 6 wt % replacement of the ATH shows the highest 50% weight loss temperature and the lowest values of the pk-HRR and the Ext Coef among all samples. Nevertheless, the LOI value and the performance in UL-94 test are not so satisfied for this sample. Figure 5 presents the TEM micrographs of the composites with 3 (EPDM/ATH/C3) and 6 wt % (EPDM/ATH/C6) replaced nanoclays. It can be observed that most of the nanoclays are well dispersed and exfoliated in EPDM/ATH/C3 sample. However, the extent of the dispersion and exfoliation of the nanoclays is less in the EPDM/ATH/C6 sample. The uneven dispersion of the nanoclays inside the EPDM matrix prevents the formation of a well-connected char structure.[21] In addition, in cone calorimeter test or TGA analysis, the specimen was placed in the aluminum plate and there was no accrual dropped from the lack of support.

Mechanical Properties

The ultimate tensile strength, elongation at break, and the modulus at 100% elongation of EPDM and EPDM/ATH composites are shown in Table V. The results show an increase of the ultimate tensile strength of EPDM with the addition of ATH, which is close to that reported in literature,[10] and a decrease of elongation at break for the EPDM/ATH relative to that of the EPDM, which is similar to the data in another study.[8] Loss of the elongation at break for EPDM/ATH is probably due to the space between the crosslinks of the polymer chains filling with a large amount of ATH, and this blocks the extension of EPDM chains during the tensile test. However, it increases the ultimate tensile strength and the modulus at 100% elongation of the composite. Addition of the nanoclay into EPDM/ATH causes the increase of the ultimate tensile strength, elongation at break, and the modulus at 100% elongation of the composite relative to those of the EPDM/ATH, and the higher nanoclay content

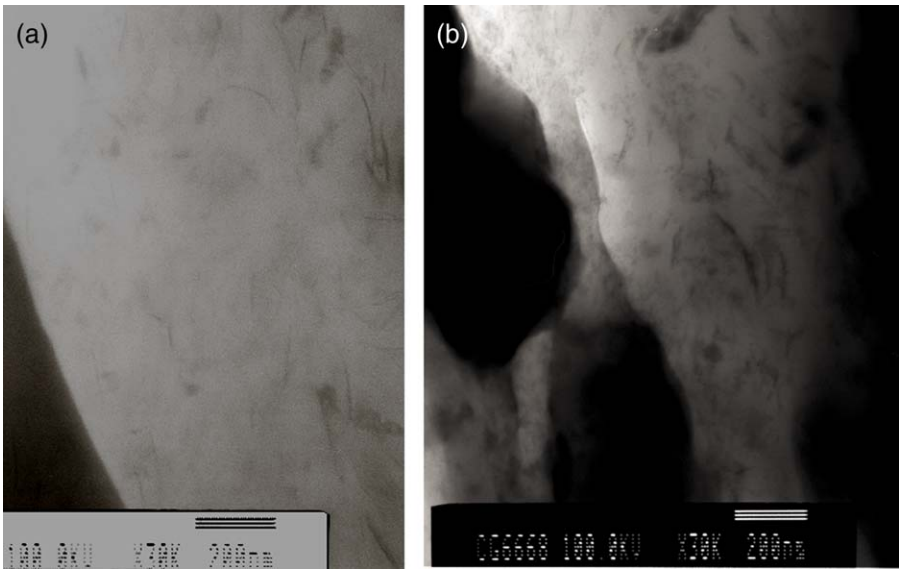

Figure 5. TEM micrographs of (a) EPDM/ATH/C3 (b) EPDM/ATH/C6 composites.

inside the EPDM/ATH composite would lead to higher mechanical properties. The high aspect ratio organomontmorillonite has been used to reinforce the EPDM material, and it identified that the EPDM molecules associate the nanoclay.[25] According to the data shown in the above article, the ultimate tensile strength, elongation at break, and the modulus at 100% elongation for EPDM composite increase from those of the EPDM by 1 MPa, 40%, and 0.5 MPa, respectively, with 6 phr nanoclay content inside the material. The increased values of the mechanical properties for the EPDM/ATH/C6 relative to the EPDM/ATH shown in Table V are similar to those reported above, and the existence of the nanoclay in the blends would improve the mechanical properties of the EPDM/ATH composites. For one more wt % replaced nanoclay inside the EPDM/ATH composite, the increments of the mechanical properties drop for sample with more than 3 wt % nanoclay. By comparing the results from TEM study, it suggests that the mechanical properties of the composites probably depend on the extent of the dispersion and exfoliation of the nanoclays.

Table V. Mechanical Properties of EPDM and EPDM /ATH Composites

Sample	Ultimate tensile strength (MPa)	Elongation at break (%)	Modulus at 100% elongation (MPa)
EPDM	4.2 ± 0.1	521 ± 6	1.3 ± 0.1
EPDM/ATH	7.2 ± 0.2	315 ± 4	1.3 ± 0.1
EPDM/ATH/C1	7.5 ± 0.2	326 ± 5	1.4 ± 0.1
EPDM/ATH/C2	7.8 ± 0.1	338 ± 2	1.5 ± 0.2
EPDM/ATH/C3	8.2 ± 0.2	346 ± 4	1.6 ± 0.1
EPDM/ATH/C6	8.4 ± 0.2	352 ± 8	1.8 ± 0.1

CONCLUSIONS

The nanoclay exhibits the synergistic flame retardancy with ATH in the EPDM/ATH/nanoclay blends. A small amount of nanoclay content (1–6 wt %) in EPDM/ATH composite would cause a better thermal stability and flame retardancy of the material than that sample without the nanoclay. This attributes the generation of a better reinforced insulating barrier based on the dispersion and exfoliation of the nanoclay in the composite matrix that restricts the diffusion of oxygen and the decomposed organic volatiles.

Results obtained from cone calorimeter and smoke density chamber tests indicate that EPDM/ATH composite samples replaced with more nanoclay allow improving the flame retardation and smoke suppression. Dispersion and exfoliation of the nanoclays inside the composites observed from TEM micrographs are better for material with lower nanoclay loading, and LOI and UL-94 measurement results are probably related to this. Improvement of the ultimate tensile strength, elongation at break, and modulus at 100% elongation has been found for the composite with more loading of the nanoclay, but the increments of the mechanical properties tend to be reduced with more than 3 wt % nanoclay inside the blends. While keeping the V-0 rating in UL-94 test and the best LOI value of the flame retardant system, the optimum amount of the nanoclay inside the composite is 3 wt %.

ACKNOWLEDGMENTS

The authors are grateful to thank Miss Qinfeng Zeng for her technical assistance in cone calorimeter tests, to thank the Walsin Lihwa Co., LTD. for providing us the smoke density chamber test, and also to acknowledge Mr. Johnny Wu and Mr. Maurice Alphonso of Plextech Co., LTD. for their support in this study.

REFERENCES

1. Ibarra, L.; Posadas, P.; Esteban-Martinez, M. *J. Appl. Polym. Sci.* **2005**, *97*, 1825.
2. Jia, S.; Zhang, Z.; Wang, Z.; Zhang, X.; Du, Z. *Polym. Int.* **2005**, *54*, 320.
3. Ehsani, M.; Borsi, H.; Gockenbach, E.; Morshedian, J.; Bakhshandeh, G. R. *Eur. Polym. J.* **2004**, *40*, 2495.
4. Brown, M. *IEEE Electr. Insul. M* **1994**, *10*, 16.
5. Davenas, J.; Stevenson, I.; Celette, N.; Vigier, G.; David, L. *Nucl. Instru. Methods B* **2003**, *208*, 461.
6. Mitra, S.; Ghanbari-Siahkali, A.; Kingshott, P.; Rehmeier, H.; Abildgaard, H.; Almdal, K. *Polym. Degrad. Stab.* **2006**, *91*, 69.
7. Nair, A. B.; Kurian, P.; Joseph, R. *Mater Design* **2012**, *40*, 80.
8. Wu, W.; Tian, L. *Appl. Mech. Mater.* **2012**, *151*, 240.
9. Sakamoto, R.; Sato, H.; Wakamatsu, K.; Hayashi, S.; Hayashi, K. *Polym. Prepr. Jpn.* **2006**, *55*, 4085.
10. Canaud, C.; Visconte, L. L. Y.; Reis Nunes, R. C. *Macromol. Mater. Eng.* **2001**, *286*, 377.
11. Canaud, C.; Visconte, L. L. Y.; Sens, M. A.; Reis Nunes, R. C. *Polym. Degrad. Stab.* **2000**, *70*, 259.
12. Alexandre, M.; Dubois, P. *Mater. Sci. Eng. R* **2000**, *28*, 1.
13. Beyer, G. *Fire Mater.* **2001**, *25*, 193.
14. Schall, N.; Engelhardt, T.; Simmler-Huebenthal, H.; Beyer, G. Rockwood Clay Additives, *Eur. Pat.* 1,183,306, March 6, **2002**.
15. Fu, M.; Qu, B. *Polym. Degrad. Stab.* **2004**, *85*, 633.
16. Szep, A.; Szabo, A.; Toth, N.; Anna, P.; Marosi, G. *Polym. Degrad. Stab.* **2006**, *91*, 593.
17. Laoutid, F.; Gaudon, P.; Taulemesse, J. M.; Lopez Cuesta, J. M.; Velasco, J. I.; Piechaczyk, A. *Polym. Degrad. Stab.* **2006**, *91*, 3074.
18. Haurie, L.; Fernandez, A. I.; Velasco, J. I.; Chimenos, J. M.; Lopez Cuesta, J. M.; Espiell, F. *Polym. Degrad. Stab.* **2007**, *92*, 1082.
19. Yen, Y. Y.; Wang, H. T.; Guo, W. J. *Polym. Degrad. Stab.* **2012**, *97*, 863.
20. Chang, Z. H.; Guo, F.; Chen, J. F.; Zuo, L.; Yu, J. H.; Wang, G. Q. *Polymer* **2007**, *48*, 2892.
21. Jiang, Y.; Zhang, X.; He, J.; Yu, L.; Yang, R. *Polym. Degrad. Stab.* **2011**, *96*, 949.
22. Lu, H.; Si, J.; Zhao, D.; Wu, H.; Ma, Y.; He, H. *Asian J. Chem.* **2012**, *24*, 4056.
23. Camino, G.; Maffezzoli, A.; Braglia, M.; De Lazzaro, M.; Zammarano, M. *Polym. Degrad. Stab.* **2001**, *74*, 457.
24. Zhang, J.; Hereid, J.; Hagen, M.; Bakirtzis, D.; Delichatsios, M. A.; Fina, A.; Castrovinci, A.; Camino, G.; Samyn, F.; Bourbigot, S. *Fire Saf. J.* **2009**, *44*, 504.
25. Chang, Y. W.; Yang, Y.; Ryu, S.; Nah, C. *Polym. Int.* **2002**, *51*, 319.